

A study on a instability slope in Taiwan subjected to rainfalls

D H Hsiao^{1*}, C S Hsieh¹, L C Yeh¹, D Y Lin¹ and V T-A Phan²

¹Department of Civil Engineering, National Kaohsiung University of Applied Sciences, 415 Chien Kung Road, Kaohsiung 80778, Taiwan R.O.C.

²Faculty of Civil Engineering, Ton Duc Thang University, Ho Chi Minh City, Vietnam

Corresponding author, E-mail address: hsiaodh@kuas.edu.tw

Abstract. After the long-term monitoring on the Chaishan area in Taiwan from 2005 to 2012 by Kaohsiung City Government, the obtained results showed that annual lateral displacements in the region are about 7-8cm to the Taiwan Strait. The geological surface profiles of Chaishan area are in sequence weathered limestone, clay layer, limestone and mudstone layer, respectively. Thus the frictional resistance between weathered soils and rock layer could decrease after infiltration of rainwater due to impervious to water of the lowest mudstone layer. Typhoon invades often Taiwan each year, resulting in rainfall infiltration and rising groundwater level, as well as increased pore water pressure within the soil mass, causing the earth movements in some parts of Chaishan, especially in the Temple A (Shan Hai Temple) accompanied with cracking phenomenon. In this paper, limit equilibrium (LE) and finite element method (FEM) are used for slope analysis, in which the slope is considered as unsaturated soil. Results showed groundwater amounts are easy to accumulate and increasing pore water pressure give resulting in decreased safety factor. Both of groundwater level and rain durations were also considered in this study.

1. Introductions

Kaohsiung Chaishan is one of the most important attractive spots in southern Taiwan due to the topography of coral reef limestone. However, due to limestone on the surface and mudstone beneath it, the rainwater can reach to the interface, so that its strength is weakened, and forms a weak surface at the interface. Hsiao et al. [1] proposed that parts of the limestone could roll down so that there is some limestones at the foot of the mountain of the Chaishan area, and its geological profiles from the ground surface was weathered mudstone layer, weathered limestone, mudstone and limestone in sequence. While continuing the research on the Chaishan area, we can find that the natural geological conditions of Chaishan are fragile and there is sustained displacement phenomenon. Jen et al. [2] identified three types of slope instability near the shore at Chaishan, including: (1) on the lower section of the slope, wave erosion exposes the mudstone and destabilizes the limestone fragments being sealed above it; (2) slumps on the re-cemented limestone fragments; (3) rock fall from cliffs near the ridge. Yang et al. [3] mentioned hydro-mechanical analysis of two unstable slopes by reducing matric suction and thus pore water pressure variations due to rain infiltration. As the effective shear strength of the sliding surface becomes smaller, the displacement of the slope gradually occurs and the slope is finally destroyed. Oh and Lu [4] analyzed two slopes in South Korea using limit equilibrium and finite element methods, of which the unsaturated part was analyzed using a suction stress characteristic curve (SSCC) and a soil



water retention curve (SWRC) slope, hydromechanical properties, shear strength and rain history. Li et al. [5] discussed the role of saturated soil during water permeability and rainfall in homogeneous slope surface damage.

Here, we first detected the monitoring data of Chaishan area from 2005 to 2012, and the apparent movements in the area are known from the data, which is more obvious during the rainfall period. In this paper, both methods of finite equilibrium (LE) and finite element method (FEM) are then used to study the changes of slope movement and safety factor according to the different rainfall intensity and groundwater level variation. Based on the changes of rainfall intensity and groundwater level, Regional slope stability and the relationship between the destruction of the interface and further explore the main cause in the Chaishan area is related to rainfall. Since super Typhoon Morakot destroyed many monitoring equipment, we selected 2010 Typhoon Fanapi as a case for rainfall analysis. The objective of the study tried to understand the failure mechanism of unsaturated slope on Chaishan after the typhoon rainfalls, and expect the results could also provide the local government as a reference for subsequent disaster prevention.

2. Study area

Figure 1 is a map of Chaishan where the study area located in. It is located in the urban area of Kaohsiung City on the southwestern side of Taiwan near the Taiwan Strait. On the left side of this area, the right side of Chaishan is called Shoushan. There is a small fishery port in the area. There are still hundreds of dwellings in Chaishan, including two colleges, Sun Yat-Sen University. The scenery is very beautiful, but there seems a potential landslide on the slopes from the past literatures [1, 2]. The geology map shown in figure 2 displays most lands of Chaishan are covered with limestones and mudstone, the latter of which is more popular seen in the western areas.

Figure 2 also shows the geological profile of Shoushan, and they are comparatively simpler geology on Chaishan. The main geology in the area is composed of a few limestone mixed with mudstone, while the pervious limestone below the surface limestone and weathered collapsible soil on the slope. Regarding the Chaishan's topography, it belongs to the dip slope. As for the thickness and distribution of weathered soil layers and the limestones, we can understand them from the boring data mentioned in the later.



Figure 1. Study area and Chaishan location map

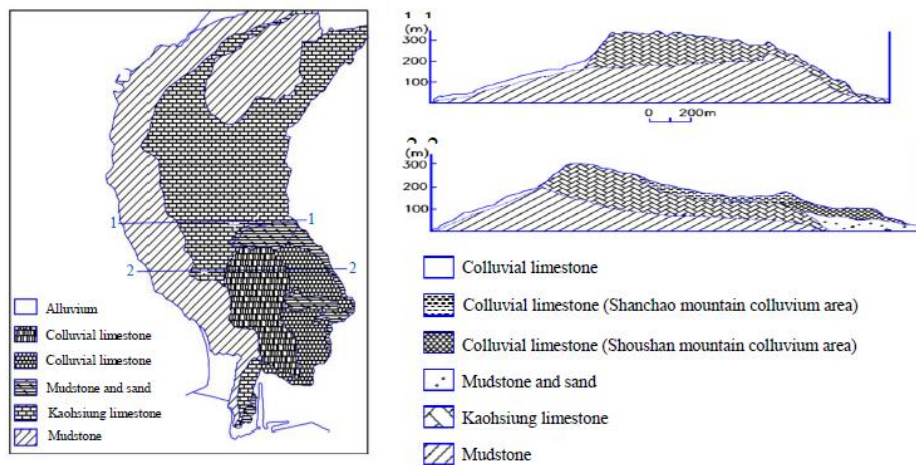


Figure 2. Shoushan geological map and geological section of the Shoushan area

Figure 3 shows the topographic map of Chaishan in Kaohsiung. The overall topography shows an east-west slope with a slope of about 20-35%. However the west side of the road seems slightly steep, possibly 40-50%, there are two temples in this area, Temple A (Shan Hai Temple) is a center for local people's beliefs, and many houses gather around these two temples. Figure 3 also shows the relevant on-site buried monitoring instruments, including drilling holes, inclinometers, piezometer, GPS stations, automatic rainfall equipment and the others, but only the inclinometers and piezometer positions are shown in the figure. A total of 21 monitoring systems, including 15 inclinometers, 6 piezometers, 15 GPS measuring stations and one automatic rainfall gauge, were set up in the zone between 2005 and 2012. At the beginning there were 18 drilling holes drilled in June 9th, after that onwards to begin monitoring. Figure 3 shows also a field investigation in site survey in the area, showing the elevation of the two sections and the Chaishan Road. The monitoring results over the long-term period (2005-2012) show that the stratigraphic slip in the area is mostly concentrated on the west side of Chaishan Road, and the displacement during the rainfall shows a significant increase. The on-site survey shows that there are obvious displacement for roads and houses in this area with obvious clearly cracks. It can be seen from the figure that there are obvious cracks and differences in height between the roads outside the houses.

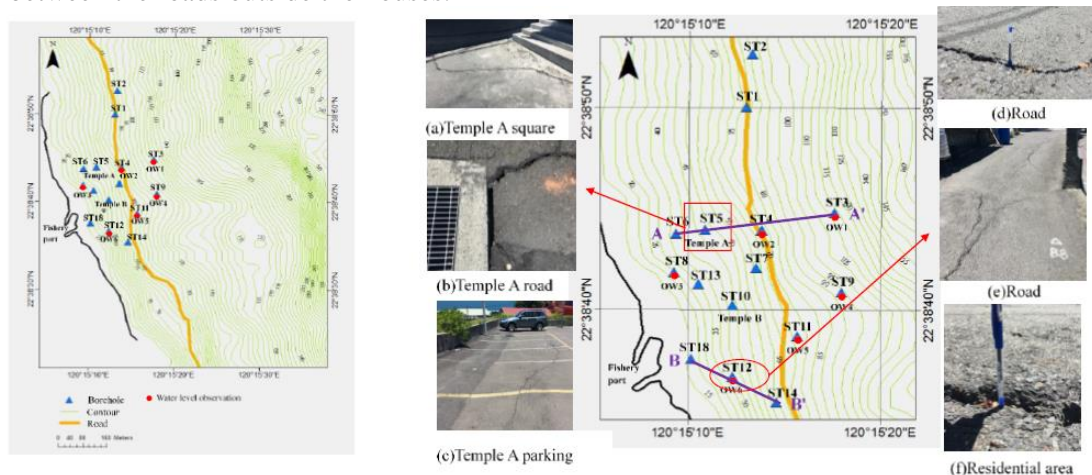


Figure 3. Topographic map (left) and field investigation (right) in site survey

Figure 4 shows the GPS and inclinometer surface displacement map between 2005 and 2012, although there are differences between the two plans but the overall road to the west side having a larger amount of displacement, as the GPS measurement is larger because there is no inclinometer

embedding resistance. The annual displacement to the Taiwan Strait in Chaishan ranges from 7 to 8 cm. In the monitoring results, great displacement was found around Temple A. Based on the monitoring data, the inclinometer number near Chaishan Fishing Port was identified as ST18, in which the thick mudstone layer is underlain, there seems to be a little bulging due to the swelling behavior of mudstone. In comparison with elevation contour diagram in figure 5, we may see clearly the actual conditions on the scene from the figure.

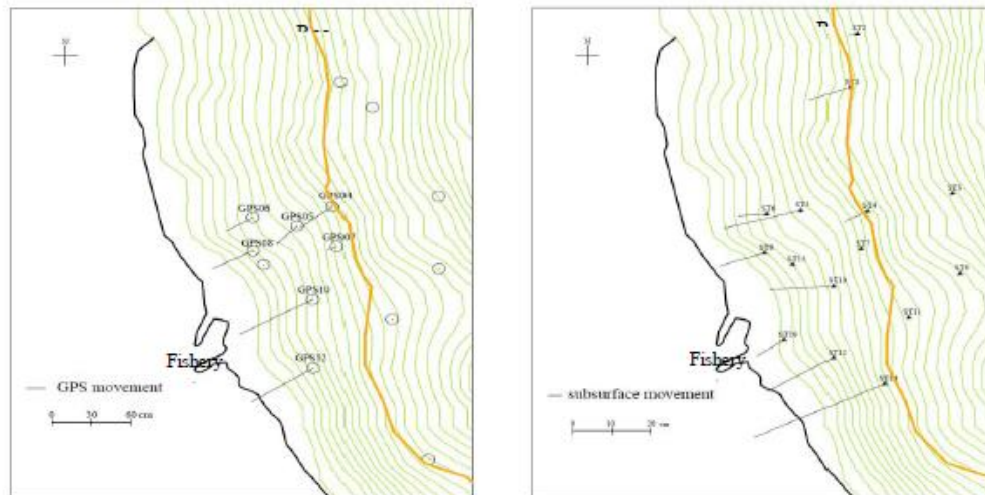


Figure 4. GPS and inclinometer displacement diagram

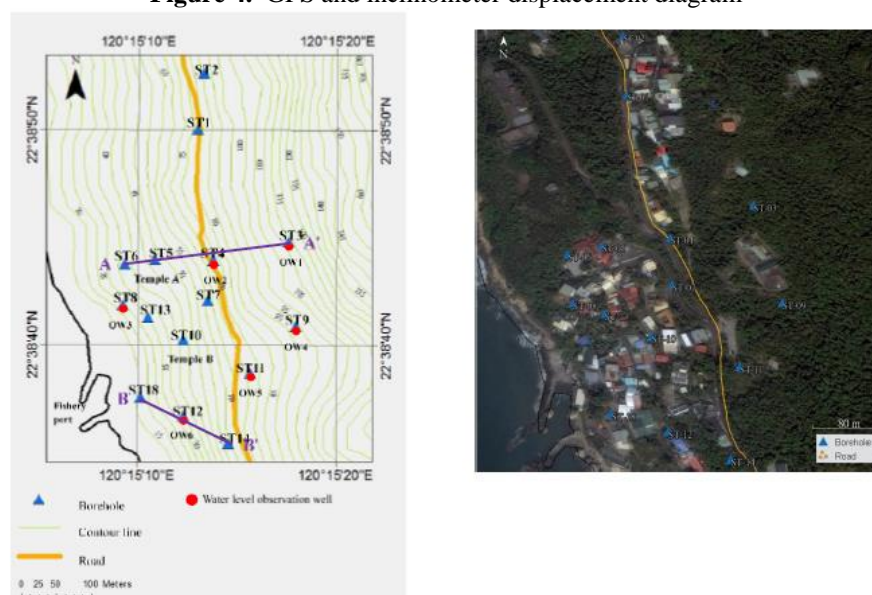


Figure 5. Elevation contour diagram and satellite picture in study area

According to the drilling data, the geological composition of the area is broadly divided into four types: mudstone, limestone, silty clay and limestone collapsible soil from the bottom to the surface. First, the drilling data are set by using the drilling holes and inclinometers in Section A-A', which extends to the east of Chaishan Road from the plaza in front of Temple A near the coast and is drawn to A-A' by ST5, ST6, BW19, BS7 and ST3 as shown below in figure 6. The figure shows also that the section is geologically impermeable to mudstone, while strata of ST5 and ST6 (around Temple A) are covered with a highly permeable limestone layer that continues over silty clay and limestone collapsible layers. Groundwater table uses water level observation wells OW1 and OW2 adjacent to

this section as a basis for analyzing the effect of groundwater level. Figure 6 shows also that the lower slope of this section is near the fishing port of Chaishan in Section B-B'.

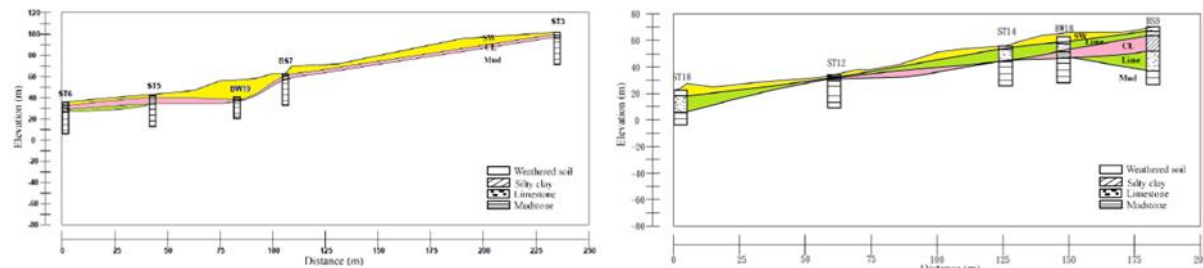


Figure 6. Distribution of soil layers in A-A' (left) and B-B' (right) section of Chaishan

Table 1 shows the accumulated rainfall during typhoon over the past years. Among them, the three typhoons during 2008-2010 caused major disasters in Taiwan and Kaohsiung. At that time, the accumulated rainfalls of Kalmaegi, Morakot and Fanapi in Chai Shan were 523.5, 726 and 554.5 mm respectively. As the local automatic rain gauge in 2009 was damaged during super Morakot disaster, the rainfall readings measured by the Fanapi typhoon in the second year after being repaired were used as the rainfall data for follow-up research. Figure 7 summarizes the changes in the groundwater levels of the monthly rainfall and piezometer OW1, OW2 and OW6 from 2005 to 2012. The groundwater level at section A-A' and section B-B' is located in the rainy season showed a clear upward trend in groundwater levels. The monitoring results show that the water table is about 0.5 to 1.5 meters below ground surface, whereas groundwater table in the dry season is about 2 to 5 meters below ground surface.

Table 1. Typhoon cumulative rainfalls over the calendar year

Years	Typhoon	Duration	Accumulated rainfalls (mm)
2005	Haitang	7/16~7/20	412
2006	Bilis	7/12~7/15	303
2007	Pabuk	8/7~8/9	30
2008	Kalmaegi	7/15~7/20	523.5
2009	Morakot	8/6~8/10	726
2010	Fanapi	9/17~9/20	554.5
2011	Nanmadol	8/27~8/31	299
2012	Talim	6/16~6/21	222.5
	Tembin	8/21~8/28	174

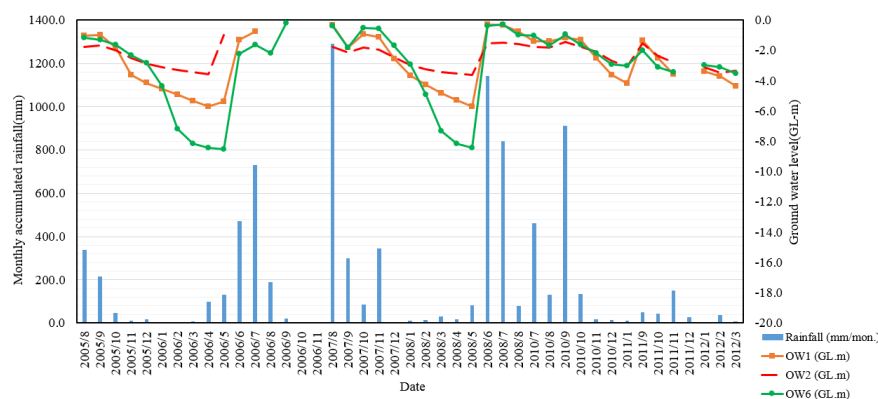


Figure 7. Monthly rainfalls and groundwater level variations from 2005 to 2012

3. Numerical simulations

In order to simulate the slope stability of the Chaishan slope during typhoon and rainfall, this paper uses the limit equilibrium (LE) and the finite element method (FEM) for slope analysis. Geo-Studio (Geoslope co.) [6] is used for the LE method as well as PLAXIS-2D (Plaxis co.) [7] is used for FEM analysis. At each stage SIMGA/W analysis is used to calculate slope stress and strain, SEEP/W analysis for seepage flow, and then the results could be put into the SLOPE/W to evaluate slope safety factor. In recent years, numerical analysis of unsaturated soils has been used extensively. The soil moisture characteristics deduced from Fredlund et al. [8], van Genuchten [9], Lu and Likos [10] and Lu et al. [11]. The empirical formulas of SWCC curve and hydraulic conductivity coefficient as shown in equations (1) and (2) were used to calculate the related soil parameters under unsaturated state of the effective stress and suction.

$$S_{eff} = \frac{\theta - \theta_r}{\theta_s - \theta_r} = \left[\frac{1}{1 + \{a(u_a - u_w)\}^n} \right]^{1-1/n} \quad (1)$$

$$k_w = k_{sat} \left[\frac{\left[1 - \{a(u_a - u_w)\}^{n-1} [1 + \{a(u_a - u_w)\}^n]^{\frac{1}{n-1}} \right]^2}{[1 + \{a(u_a - u_w)\}^n]^{\frac{1}{2} \cdot \frac{n}{2}}} \right] \quad (2)$$

However, the soil shear strength in the unsaturated state could be written as Equation (3). The method defined according to the Mohr-Coulomb failure criterion was used to describe or predict the nonlinear relationship between soil shear strength and suction (Qi and Vanapalli [12]). Based on the Mohr-Coulomb failure criterion and the ultimate stress method, the slope safety factor is calculated as Equation (4). This study uses the SLOPE/W and PLAXIS software to calculate the safety factor of slope. The former obtained by the theory of limit equilibrium method, as shown in equation (4); but the latter is different from the limit equilibrium method. Thus performing calculation of finite element method, the re-calculation of the safety factor results will be chosen. In order to consider the convenience of numerical operations, soil strength parameters $\tan\theta$ and c were usually used and gradually decrease until the slope occurs damage for shear strength reduction method, the value obtained is the slope of the reduction value used to indicate the safety factor as shown in equation (5).

$$\tau_f = c' + (\sigma - U_a) * \tan \phi' + \{S_{eff}(U_a - U_w)\} * \tan \phi' \quad (3)$$

$$FS = \frac{c' + \sigma' \tan \phi'}{W * \sin \alpha * \cos \alpha} \quad (4)$$

$$M_{sf} = \frac{\tan \phi_{input}}{\tan \phi_{reduced}} = \frac{c_{input}}{c_{reduced}} \quad (5)$$

The depth of soil layer in each section is plotted by drilling boring data. The section model built by PLAXIS-2D is shown in figure 8. The degree of mesh densification is very tight, however, due to the boundary effect, the extension of the two cross sections will be evaluated separately. The section A-A' has a total length of 235 meters, an upper slope of 101 meters and a lower slope of 35 meters, with a grid number of 15789; a section B-B' of 185 meters in length and an upper slope of 70.2 meters, The lower slope is 22.9 meters high with 4801 grids, while the two sections extend horizontally outward to 500 meters due to the boundary effect.

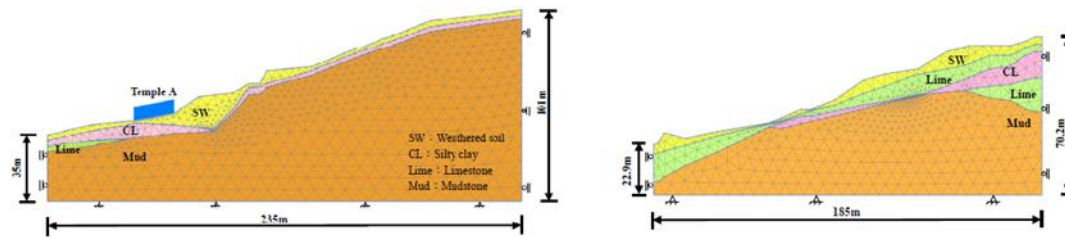


Figure 8. PLAXIS section model in A-A' and B-B'

In this case, we use three sets of modules to analyze slope stability, SIMGA/W, SEEP/W and SLOPE/W. Since the software model can be applied to other modules only once, The parameters of the module input materials can be analyzed, as the software used to specify the destruction of the surface out of the entrance range, so do not need to consider the boundary effect of the problem, figure 10, respectively, are A-A' section and B-B' sectional model.

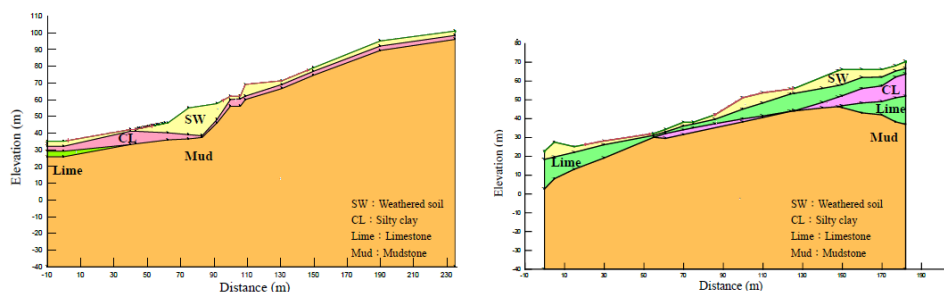


Figure 9. SLOPE/W section cross section model in A-A' and B-B'

According to the field survey data, the water table readings of six buried holes were conducted in the Chaishan area in 2005. The water table of OW1 and OW2 adjacent to the section A-A' and the OW6 groundwater table of section B-B' measurement data is used as an assessment of the groundwater level assumptions. According to the monitoring data, the groundwater level at the two cross sections was at an average water table of about 1.5 to 2.0 meters below the surface during September 2010. Therefore, a groundwater table setting of 2.0 meters below ground surface will be used as a design groundwater table as the basis. Table 2 and 3 are the material parameters of the soil layers in sections A-A' and B-B', respectively. Due to a lot of parameters, the sensitivity analysis of the parameters will be performed later in this study, including the value of shear strength c , internal friction resistance ϕ angle and permeability coefficient k value of weathered soil and understanding they affect the slope safety factor and displacement.

Table 2. A-A' section soil parameters

Layer	SOIL/ROCK	γ_m kN/m ³	γ_{sat} kN/m ³	E' kPa	ν	c kPa	S_u kPa	ϕ' (°)	ψ (°)	k_x m/day	k_y m/day
I	Weathered soils	21	22	34000	0.35	20	-	20	0	1.063	1.063
II	Clay	20	21	13545	0.35	-	30	15	0	4.75×10^{-3}	4.75×10^{-3}
III	Limestone	20	21	350000	0.18	500	-	22	0	1.063	1.063
IV	Mudstone	21	22	52000	0.40	-	50	30	0	8.64×10^{-4}	8.64×10^{-4}

Table 3. B-B' section soil parameters

Layer	SOIL/ROCK	γ_m kN/m ³	γ_{sat} kN/m ³	E' kPa	ν	c kPa	S_u kPa	ϕ' (°)	ψ (°)	k_x m/day	k_y m/day
I	Weathered soils	21	22	34000	0.35	20	-	20	0	0.2497	0.2497
II	Limestone	20	21	350000	0.18	500	-	22	0	0.2497	0.2497
III	Clay	20	21	13545	0.35	-	30	15	0	4.75×10^{-3}	4.75×10^{-3}
IV	Mudstone	21	22	10000	0.40	-	50	30	0	8.64×10^{-4}	8.64×10^{-4}

4. Results and discussions

According to the analysis by Hsiao et al. [1] on the slopes in Chaishan region in 2015, the geological conditions in the Chaishan region are fragile and displaced during rainy season. Therefore, in the contour map of Chaishan region, the sections A-A' and B-B' section, the comparison between the change of slope safety coefficient and displacement under rainfall simulation and the monitoring displacement of section A-A' during Fanapi Typhoon. The section A-A' is selected because it is close to Temple A, which has a history of three hundred years of cultural history. Local residents live near the area for many times and there are obvious cracks in the roads near the area after the site survey. The B-B' section was selected due to the relatively low elevation of the area and its proximity is to Chaishan Fishing Port. The boring data show that the geology of the area consists mainly of limestone and impermeable mudstone with higher water permeability. Therefore, rainwater and groundwater level permeability and accumulation of the rainfalls on the surface of mudstone may cause the phenomenon of softening and swelling of mudstone.

4.1. Effect of shear strength parameters c and ϕ on slope safety factor

According to the cross section A-A', it is found that the section is thicker and forms like a bowl-shaped structure in the rear of Temple A, and is connected with silty layers and silty clay layers. The sliding surface of the area can be mainly located at the interface between the collapsible soil and the silty clay layer. Therefore, using the SLOPE/W analysis, the c values of the collapsed soil layer A-A' are defined as 20-35 kN/m² and then ϕ angles are 10°-45°, the variation of the safety factor is calculated. Figure 10 shows the safety factor for slope with different values of c and ϕ for the clayey soil. The table shows that when $c = 20$ kN/m² and $\phi = 10^\circ$, the FS = 0.93 and the ϕ angle continuously increases FS = 1.32 at $\phi = 30^\circ$. Although the soil cohesion increases but the angle ϕ remains constant, the slope is still unable to resist. It can be clearly seen from the figure that when c and ϕ increase, the safety factor of the slope tends to increase. However, when $c = 30$ kN/m² and $\phi = 30^\circ$, there is a decrease of FS = 1.4 of the slope after calculation due to the phenomenon that the safety factor is decreased due to the transformation of the failure surface of the slope, which can be seen from the figure 11, the failure surface of the slope changes from arc-shaped dotted line to solid line. The reason for the decline is that the failure surface is transferred from the soil layer to the silty clay layer, as shown in figure, however, ϕ angle of the silty clay layer is smaller, so the worse after sectioning.

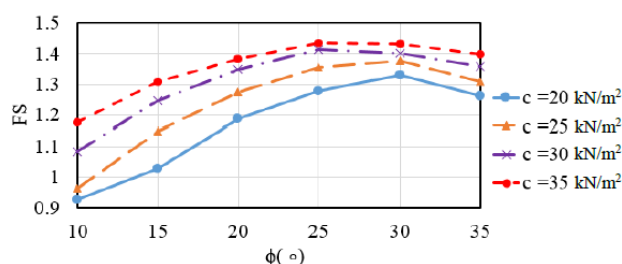


Figure 10. Changes of the safety factor owing to c and

ϕ

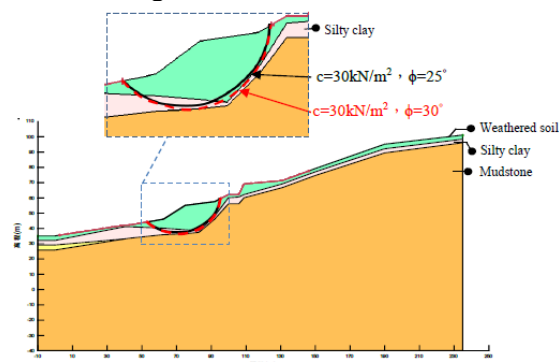


Figure 11. Change of the sliding surface for A-A'

section

4.2. Effect of permeability on slope safety factor

Li et al. [5] pointed out that rainfalls and saturated permeability may be related to the rise of groundwater table or the increase of pore water pressure in the soil due to the failure mechanism of the slope, so the first two factors of rainfall duration and soil permeability will affect slope damage surface location and type of results. Although the overburden of mudstone above the B-B' section is only 10-m-thick weathered soil layers and limestone, due to the large number of limestone holes and

better water permeability in this area, by replacing the collapsed soil layer with limestone. The permeability coefficient of the soil layer is discussed to affect the change of the slope safety factor when the rainfall comes. The permeability coefficient is first set from 0.8m/day to 1.5m/day. Figure 12 shows that the coefficient of permeability of collapsible soil layer is $k = 0.8\text{m/day}$, the $FS = 1.78$, however, when the rainfall persists and the rainfall continues for 4 hours, FS of the section will decrease to 0.89 and then breaks down. It can be clearly seen from the figure that on the contrary when the k value of the collapsed soil layer is larger, the rainfall has little effect on the safety factor of the slope because the surface soil rainwater can be quickly removed and the dangerous hazard to the slope is relatively low.

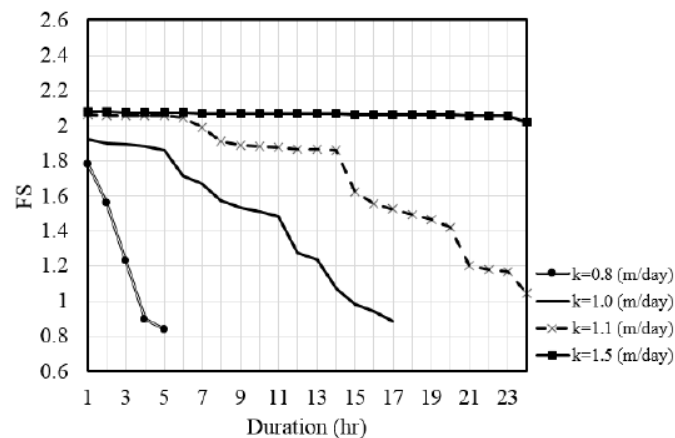


Figure 12. Different values of k impact on the safety factor for B-B 'cross-section

4.3. Effect of slope damage surface location on safety factor

Firstly, this study sorted out the monitoring data of each inclinometer over the years and extracted some data to provide the range of failure surface to explore the influence on the safety factor. Figure 13 is a displacement map using the inclinometer ST6, ST5 and ST3 for the section A-A'. Monitoring data show the location of the destruction of the surface, roughly draw a group of slope slip surface, and then use SLOPE/ W analysis of each group of sections of the safety factor.

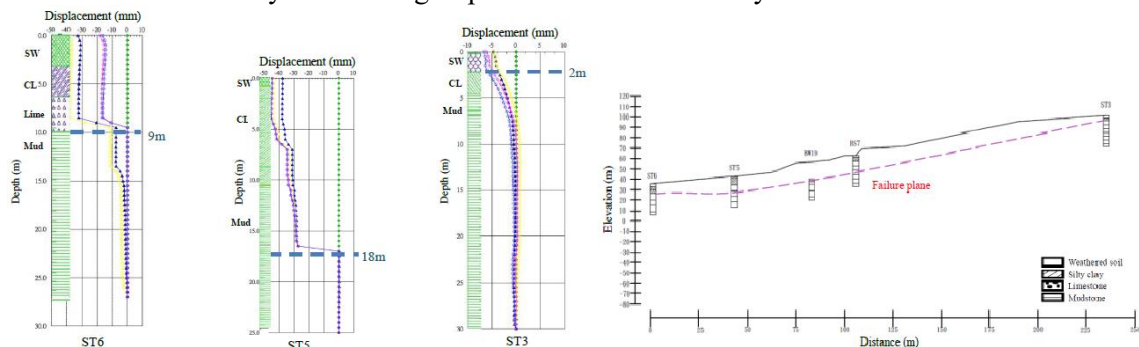


Figure 13. the inclined tube displacement and sliding surface position in A-A 'cross-sectional

The results of the analysis are shown in figure 14, in which figure 14(a) shows the safety factor for the fully specified failure surface of section A-A', where the green border is the slope sliding surface area. However, the factor of safety will overestimate the overall stability of the slope due to the fact that the slope may first be destroyed elsewhere. Therefore, in figure 14(b), the setting of the entry and exit of the failure surface, to find out the safety factor of the slope in the critical state. In the figure, the green arc-shaped checkered area is the area of failure surface of the section. Both of the above two methods belong to the boundary of the failure surface, Therefore, in figure 14(c), PLAXIS software is used to evaluate the overall slope reduction factor, and the safety factors of the three conditions are

summarized in Table 4. The results show that using different methods to calculate the safety factor of slope varies greatly, among which, the failure surface $FS = 1.94$ is completely specified. Since this failure surface is a sliding surface drawn according to the failure section of each inclinometer, when SLOPE/W is calculating the safety factor sliding will only be made using this sliding surface, so the result may be significantly higher than the other two. $FS = 1.07$ shows the process of calculating the damage surface. The software calculates the node on the entrance and exit repeatedly and calculates the critical damage of the slope, however PLAXIS considers the overall displacement of section A-A' and reduces the angle ϕ until the failure of the slope, which results in a slope FS of 1.06.

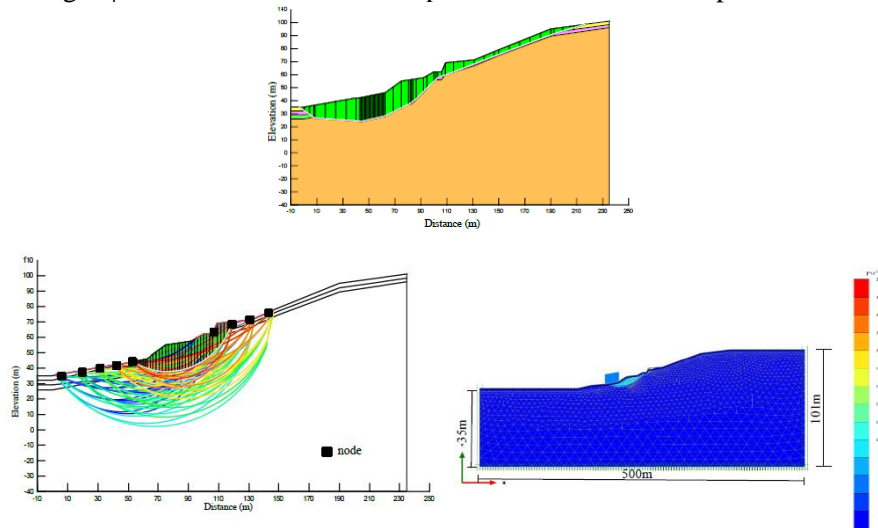


Figure 14. (a) completely designates, (b) designated A-A' section out of the entrance damage, and (c) PLAXIS for the failure plane A-A'

Table 4. Safety factor for three events in A-A' section

Completely designates the failure plane (SLOPE/W)	Designated A-A' section out of the entrance damage (SLOPE/W)	PLAXIS
1.94	1.07	1.06

As mentioned above, the section B-B' extends from the inclinometer at Chaishan fishing port at ST18 to the station ST12 at the residential area of Chai Shan tribe and finally to Chaishan Road at the inclinometer no. ST14. Table 5 using different calculation methods is quite different. In addition, the safety factor obtained from the above section B-B' compared with that from section A-A', the results show that section A-A' in Chaishan is more dangerous.

Table 5. Safety factor for three events in B-B' section

Completely designates the failure plane (SLOPE/W)	Designated A-A' section out of the entrance damage (SLOPE/W)	PLAXIS
2.68	2.07	1.32

4.4. Effect of various groundwater tables on the slope failure

Due to the special geological conditions of Chaishan, this paper simulates the failure of slopes A-A' under different groundwater levels and rainfall respectively. However, in order to find out the main failure area of slope, two rainfall intensity data for analysis rainfall intensity 5mm/hr and continuous rain for 24 hours. Since the monitoring results are in the range of 1-2m stated before over the years, the groundwater table is set as 2 meters below the ground surface. In addition, the depth of the

mudstone in the section discussed is about 10 meters below the surface. Therefore, the groundwater is also located at a depth of 10 meters below the earth's surface. The result of figure 14 shows that the main displacement area is around Temple A. The simulation results show that the groundwater is located 2 meters below the surface. This may be due to the fact that the influence area reaches to 15-meter-thick silty clay layer, probably because its own drainage is not easy and existence of poor permeability of mudstone underlain below, resulting in rainwater infiltration in this area. As for 10 meters below the ground surface of figure 15, we can observe that the displacement of this area is small. The overall finding is that displacement at -2m is much larger than those at -10m.

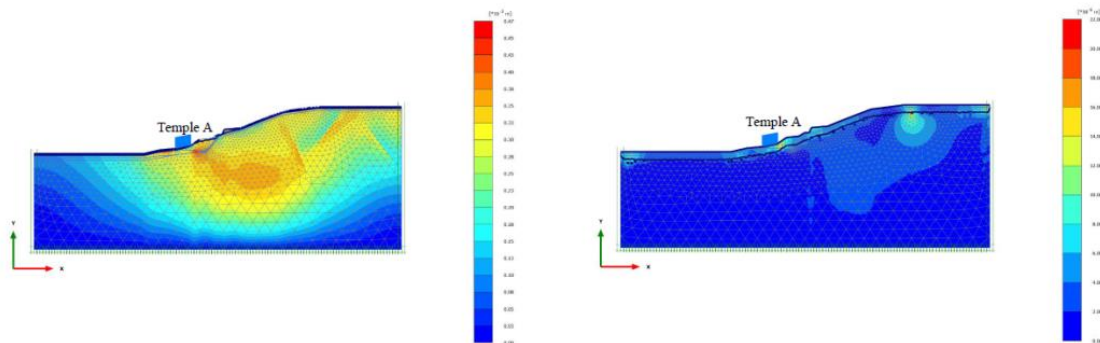


Figure 15. The displacement chart of the slope when groundwater level -2m and -10m

4.5. Typhoon rainfalls affect the slope safety

In order to investigate the relationship between the main causes of slope-slip and the rainfall in Chaishan, this study uses the rainfall readings measured during the Fanabi typhoon in 2010. Through the analysis of the stability of slope A-A' in Chaishan by PLAXIS and SLOPE/W software, and plot the relationship between time duration and the rainfall during the typhoon period in figure 16 and the groundwater level variation by the piezometer OW1 and OW2 adjacent to the A-A' section. The figure shows OW1 groundwater level gauge change trend is obvious, because the region geological collapse of the soil layer is relatively thin, and then take about 1.5-3m thick silty clay, so the rain can't be quickly excluded, and in this formation of temporary habitat groundwater; OW2 underground water level meter in the rear of the Temple A, the collapse of soil in this area about 19m thick, so the upward trend of groundwater level is less obvious. Further use of SLOPE/W analysis, where the A-A' section safety factor changes during typhoon, the results are shown in figure 17. In this figure, it is seen that the safety factor gradually decreases along the A-A' section during the typhoon Fanapi than during the typhoon. However, at 4:00 pm on September 19, local time, Than the highest rainfall intensity in the typhoon, the rainfall intensity as high as 86.5 mm/hr, it is clear from the figure that the section of the safety factor at this moment also significantly decreased phenomenon. Yang et al. [3] mentioned that the increase of cumulative rainfall led to a decrease of the safety factor, which may be related to that the p'-q' graph is close to K_f -line.

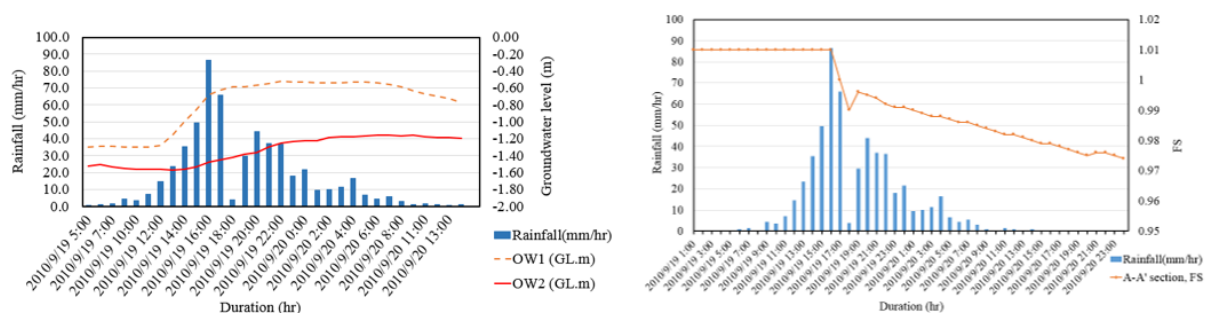


Figure 16. Variation of groundwater level during Vanaipi typhoon

Figure 17. Change of safety factor for A-A' section during the Typhoon

5. Conclusions

- The geology of limestone in Chaishan, Kaohsiung is not entirely composed of water-permeable limestone and impervious mudstone. This study indicates that it is possible that limestone from the top hills had collapsed and rolled down the Chaishan area under the influence of topography or natural forces. However, the collapsed limestone may mix with the fragments and inclusions of weathered sands and clayey soils.
- After finite equilibrium (LE) and finite element method (FEM) are used for slope analysis, the results of two-section simulation analysis are satisfactory with unsaturated soil considered. Parameters sensitivity analysis such as shear strength c value and ϕ angle, collapsible soil water permeability coefficient k value were performed. It is found that the location of failure plane will affect the safety of the slope very significantly. Through the simulation for A-A' and B-B' section, the results showed that the A-A' of the Chaishan area is more dangerous than the section B-B'.
- The result of inclinometer shows that the main sliding surface of the slope in Chaishan area is mostly located at the interface of weathered soils, limestone and mudstone. Using different rainfall intensities and the groundwater level of -2 m and -10 m, the results show that the section A-A' is at the inclinometer ST5 near Temple A. Due to the thick silty clay and poor drainage, water level is accumulated.

References

- [1] Hsiao DH, Phan TAV, Kung TC, and Liao CJ 2015 Investigation and assessment of a landslide case study in southwestern Taiwan. *Disaster Advances*. **8**(4) 39-52.
- [2] Jen CH, Chen JH, Lei HF, Ho LD, Zhou HW, Lin TY, Lu CH, Hsueh MY, Chyi SJ 2018 Recent movement of the Late Pleistocene Shoushan slump, southwestern Taiwan, based on landform surveys. *Quaternary International*. (In press)
- [3] Yang KH, Uzuokab R, Thuoa JN, Lina GL, Nakaib Y 2017 Coupled hydro-mechanical analysis of two unstable unsaturated slopes subject to rainfall infiltration. *Engineering Geology*. **216** 13-30.
- [4] Oh S, Lub N 2015 Slope stability analysis under unsaturated conditions: Case studies of rainfall-induced failure of cut slopes. *Engineering Geology*. **184** 96-103.
- [5] Li WI, Lee LM, Cai H, Li HJ, Dai FC, Wang ML 2013 Combined roles of saturated permeability and rainfall characteristics on surficial failure of homogeneous soil slope. *Engineering Geology*. **153** 105-113.
- [6] Geo-slope International Ltd 2015 *Geo-Studio*. Canada.
- [7] Plaxis B.V. Co 2016 *PLAXIS*. Netherlands.
- [8] Fredlund DG, Morgenstern NR, and Widger RA 1978 The shear strength of unsaturated soil. *Canadian Geotechnical Journal*. **15**(3) 313-321.
- [9] Van Genuchten MT 1980 A closed-form equation for predicting hydraulic conductivity of unsaturated soils. *Soil Sci Soc Am J*. **44**(5) 892-898.
- [10] Lu N, and Likos WJ 2006 Suction stress characteristic curve for unsaturated soil. *Journal of Geotechnical and Geoenvironmental Engineering*. **132**(2) 131-142.
- [11] Lu N, Godt., JW, and Wu DT 2010 A closed-form equation for effective stress in unsaturated soil, *Water Resour. Res.* **46**(5) 1-14
- [12] Qi S, Vanapalli S K 2015 Hydro-mechanical coupling effect on surficial layer stability of unsaturated expansive soil slopes. *Computer and Geotechnics*. **70** 68-82.